Journal of Alloys and Compounds 504S (2010) S256–S259

Contents lists available at ScienceDirect

Journal of Alloys and Compounds

journal homepage: www.elsevier.com/locate/jallcom

Effect of high magnetic field on crystallization of $Zr_{46.75}Ti_{8.25}Cu_{7.5}Ni_{10}Be_{27.5}$ bulk metallic glass

Y.X. Zhuang*, J. Chen, W.J. Liu, J.C. He

Key Laboratory of Electromagnetic Processing of Materials (EPM), National Education Ministry, P.O. Box 314, Northeastern University, Shenyang, 110004, PR China

ARTICLE INFO

Article history:
Received 4 July 2009
Received in revised form 18 January 2010
Accepted 25 February 2010
Available online 3 March 2010

Keywords:
High magnetic fields
Metallic glass
Phase transition
Crystallization

ABSTRACT

It has been demonstrated that high magnetic field is a very powerful tool in controlling microstructures of materials. In this work, the effect of high magnetic field on the crystallization of $Zr_{46.75}Ti_{8.25}Cu_{7.5}Ni_{10}Be_{27.5}$ bulk metallic glass has been investigated. The isothermal crystallization of the bulk metallic glass was performed at the temperatures ranging from 643 to 713 K with or without a high magnetic field. The direction of the magnetic field is parallel or perpendicular to the sample surfaces. The annealed samples were characterized by X-ray diffraction and differential scanning calorimeter. It has been found that the crystallization of the bulk metallic glasses depends not only on the annealing temperatures, but also on the direction and the intensity of the high magnetic field. The high magnetic field significantly retards the crystallization of the bulk metallic glass at certain annealing temperatures. The possible mechanisms of high magnetic field effect on the crystallization have been discussed.

1. Introduction

With the development of superconducting magnet technology, high magnetic fields up to more than 10 T have been widely used to control the microstructures of materials during material processing such as solidification, electrodeposition and some solid–solid phase transformations [1]. Materials science in high magnetic field has attracted much attention in material design and production.

Crystallization of metallic glasses is of importance in understanding mechanisms of phase transformations far from equilibrium, evaluating the glass forming ability of the melts and producing controlled ultrarefined microstructure. The crystallization behavior of the metallic glasses is affected significantly by various factors, such as annealing temperature and time, external electric field, and high pressure [2–6]. It has been demonstrated that the high magnetic filed is also a powerful tool to affect crystallization process of metallic glasses and texture formation of the crystallized phase [7–15]. In 1987, Wolfus et al. [7] investigated crystallization kinetics of $Fe_{83}B_{12}Si_5$ amorphous ribbon under external magnetic field, and found that the growth rate of magnetic crystalline phases increased with the magnetic field. In 1990, Otani et al. [8] reported that a magnetic field of 0.3 T slightly enhanced the development of a texture formed in the crystallized $Pr_2Co_{14}B$ amorphous ribbon, in which the easy magnetization *c*-plane oriented along the direction of applied magnetic field. In 2004, Wang et al. [9] found that the isothermal crystallization of the $Zr_{62}Al_8Ni_{10}Cu_{17}$ bulk metallic glass was significantly retarded under high magnetic fields. Recently, Tsurekawa and co-workers [11–14] investigated the effect of magnetic crystallization on texture evolution in Fe–Si–B–(Nb–Cu), and found that a sharp {1 1 0} texture was formed by applying a 6 T magnetic field in a direction parallel to the ribbon surface, meaning that the high magnetic field enhances the development of the {1 1 0} texture in the crystallized α-Fe(Si) from Fe–Si–B–(Nb–Cu) amorphous alloys. However, the different mechanisms of the texture formation were suggested for Fe–Si–B and Fe–Si–B–Nb–Cu amorphous alloys, i.e. preferential growth of {1 1 0}-oriented nuclei for the Fe–Si–B amorphous alloy, and preferential nucleation for {1 1 0}-oriented grains for the Fe–Si–B–Nb–Cu amorphous alloy. Zhang et al. also found that the applied magnetic field has an evident effect on the average grain size of the phases precipitated from the Fe–Pt–B amorphous alloy [14].

Recently, we have investigated the effect of high magnetic field on the crystallization of some Zr-based bulk metallic glasses. Though it has been found that the high magnetic field has no obvious effect on the crystallization process of $Zr_{60}Cu_{20}Al_{10}Ni_{10}$ bulk metallic glass at the experimental conditions investigated [15], we do observe the great effect of high magnetic field on the crystallization of Zr–Ti–Cu–Ni–Be bulk metallic glass. In this paper, magnetic crystallization behavior of the $Zr_{46.75}Ti_{8.25}Cu_{7.5}Ni_{10}Be_{27.5}$ (Vit4) bulk metallic glass was reported.

* Corresponding author. Tel.: +86 24 83685996; fax: +86 24 83681758.
E-mail address: yxzhuang@epm.neu.edu.cn (Y.X. Zhuang).

0925-8388/$ – see front matter © 2010 Elsevier B.V. All rights reserved.
doi:10.1016/j.jallcom.2010.02.166

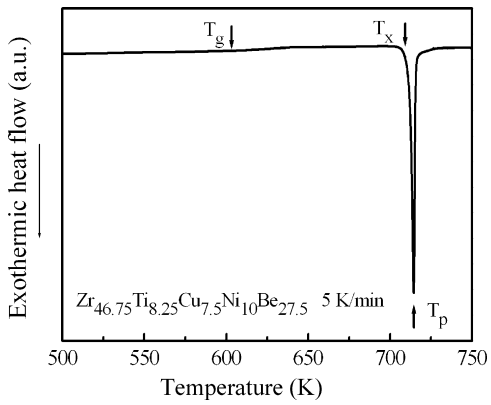

Fig. 1. DSC trace for $Zr_{46.75}Ti_{8.25}Cu_{7.5}Ni_{10}Be_{27.5}$ bulk metallic glass at a heating rate of 5 K/min.

2. Materials and methods

The ingots, with nominal composition $Zr_{46.75}Ti_{8.25}Cu_{7.5}Ni_{10}Be_{27.5}$, were prepared by melting a mixture of pure elements in a titanium-gettered argon arc furnace, then remelted in a vacuum-sealed quartz tube and quenched in water to get an amorphous rod with a diameter of 8 mm. The amorphous nature as well as homogeneity of the rod was ascertained with X-ray diffraction (XRD). Slices with a thickness of 0.5 mm were cut from the amorphous rod for differential scanning calorimeter (DSC) measurements and magnetic field annealing. The DSC measurements were carried out under a purified Ar atmosphere in a TA Q100 at a heating rate of 5 K/min. The calorimeter was calibrated for temperature and energy with high purity indium. The values of the glass transition temperature T_g, the onset temperature T_x, and the crystallization peak temperature T_p were determined from the DSC traces with an accuracy of ±1 K.

The magnetic field annealing was performed in a vacuum furnace, where a superconducting magnet (JMTD-12 T100, JASTEC, Japan) was used to generate a magnetic field with a maximum magnetic flux density up to 12 T at the center of a bore (100 mm in diameter). Detailed information about the magnetic field annealing furnace refers to Ref. [16]. The 20-mm-length isothermal region of the furnace has an accuracy of around ±3 K. The stable homogeneous magnetic fields were used in this work. For each experimental condition, amorphous slices were put into an alumina crucible (10 mm in diameter), which is centered at the place with the maximum magnetic flux density. The surfaces of the slices were either perpendicular or parallel to the direction of the magnetic field. The working vacuum is better than 2×10^{-3} Pa. After the magnetic field was applied, the samples were heated to a given temperature at a heating rate of 5 K/min, kept for a certain time, and cooled down to temperature below 100 °C in the furnace. The variation of the temperature during isothermal annealing was controlled in the range of ±0.3 K unless it was mentioned in the text. The average cooling rate is around 6 K/min. Then the samples were characterized by XRD (X'Pert Pro diffractionmeter, Cu Kα radiation) and DSC.

3. Results and discussions

Fig. 1 gives DSC trace obtained for as-prepared $Zr_{46.75}Ti_{8.25}Cu_{7.5}Ni_{10}Be_{27.5}$ bulk metallic glass at the heating rate of 5 K/min, which coincides with the heating rate used for the magnetic field annealing. The DSC trace exhibits the endothermic characteristics of a glass transition followed by an exothermic crystallization reaction at higher temperature. The glass transition temperature (T_g), the onset crystallization temperature (T_x), and the peak crystallization temperature (T_p) are 603, 712, and 714 K, respectively. Thereby, the annealing temperatures are selected in the range of 643–713 K.

Fig. 2 summarizes XRD patterns of the $Zr_{46.75}Ti_{8.25}Cu_{7.5}Ni_{10}Be_{27.5}$ bulk metallic glass annealed at 650 K for 40 min under the 0 and 12 T applied magnetic field with direction perpendicular (H⊥S, Fig. 2a) or parallel (H//S, Fig. 2b) to the sample surfaces. Please note that the variation of the annealing temperature is rather large (about ±9 K) for the experiments shown in Fig. 2. Since the position of the samples, whose surfaces are parallel to the magnetic field, is different from that of the samples with surfaces perpendicular to the magnetic field, the real annealing temperatures of two types of sample might have some difference. Therefore, no comparisons have been made between XRD patterns shown in Fig. 2(a) and (b). It is observed from Fig. 2(a) that some crystalline Bragg peaks appear whether the high magnetic field (H⊥S) was applied or not. These Bragg peaks can be indexed to the cubic $NiTi_{0.6}Zr_{0.4}$ phase and the cubic $NiTi_2$ phase. It is clear that the Bragg peaks corresponding to the $NiTi_{0.6}Zr_{0.4}$ phase become weaker when the 12 T high magnetic filed (H⊥S, Fig. 2a) was applied. However, when the magnetic field is parallel to the surfaces of the slices (H//S), the intensity of the Bragg peaks corresponding to the $NiTi_{0.6}Zr_{0.4}$ phase is enhanced under the high magnetic filed as shown in Fig. 2(b). It has also been found that there is no obvious difference between the DSC traces (not shown) of the $Zr_{46.75}Ti_{8.25}Cu_{7.5}Ni_{10}Be_{27.5}$ alloys annealed under the 0 T and 12 T high magnetic field, which is parallel to the sample surface. Apparently, the direction of the applied magnetic field shows different effect on the precipitation of $NiTi_{0.6}Zr_{0.4}$ phase, that is, the peak intensity of $NiTi_{0.6}Zr_{0.4}$ phase is enhanced for the sample surface parallel to the high magnetic field, and is reduced when the applied magnetic field is perpendicular to the sample surfaces. However, the reason is still unclear. More Bragg peaks appear on the diffraction patterns (not shown) of the samples annealed at higher temperatures (the variation of the annealing temperature is also around ±9 K). The Bragg peaks can be indexed to the $NiTi_{0.6}Zr_{0.4}$, $NiTi_2$, Zr_2Cu, Be_2Zr and unidentified phases.

Fig. 3 shows XRD patterns of the as-prepared $Zr_{46.75}Ti_{8.25}Cu_{7.5}Ni_{10}Be_{27.5}$ bulk metallic glass and the samples annealed at 688 K and different combinations of annealing time and magnetic field parallel to the sample surface. Unlike the conditions used for the experiments illustrated in Fig. 2, the

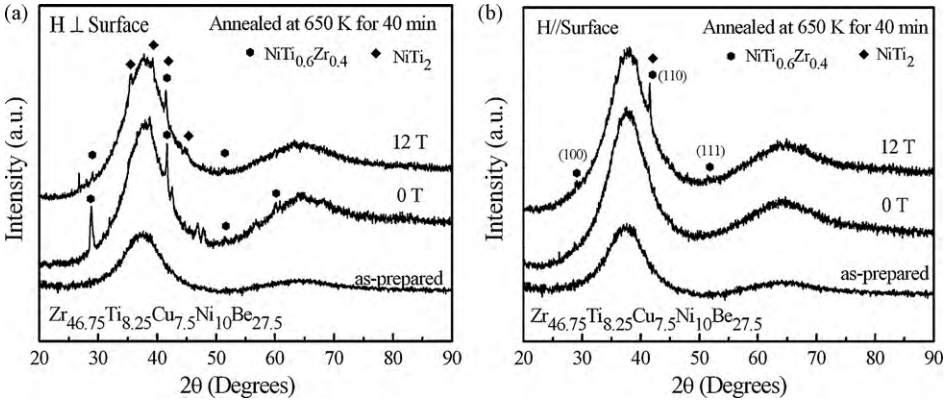

Fig. 2. XRD patterns of the as-prepared $Zr_{46.75}Ti_{8.25}Cu_{7.5}Ni_{10}Be_{27.5}$ bulk metallic glass and the samples annealed at 650 K for 40 min under applied magnetic field, whose direction is perpendicular (a) or parallel (b) to the sample surfaces.

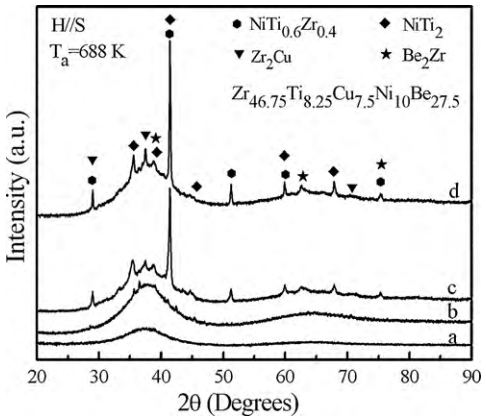

Fig. 3. XRD patterns of the as-prepared $Zr_{46.75}Ti_{8.25}Cu_{7.5}Ni_{10}Be_{27.5}$ bulk metallic glass (a) and the samples annealed at 688 K and different conditions: (b) 20 min with the 12 T high magnetic field; (c) 20 min without high magnetic field; (d) 40 min with the 12 T high magnetic field. The direction of the magnetic field is parallel to the sample surfaces.

variation of the temperature during the isothermal annealing is very small (within ±0.3 K). The XRD pattern of the sample annealed at 688 K for 20 min without magnetic field (curve c) shows obvious Bragg peaks of $NiTi_{0.6}Zr_{0.4}$, $NiTi_2$, Zr_2Cu and Be_2Zr phases, superimposed on the broad diffuse scattering peak from the amorphous phase. While only a few very tiny Bragg peaks have been found on the diffraction pattern of the sample annealed at 688 K for 20 min under the 12 T high magnetic field (curve b). It is clear that the crystallization kinetics of the $Zr_{46.75}Ti_{8.25}Cu_{7.5}Ni_{10}Be_{27.5}$ bulk metallic glass is significantly retarded at 688 K by applying high magnetic field. Under the 12 T high magnetic field, longer annealing time induces the appearance of the obvious Bragg peaks (refer to curve d), whose positions are same with those found from curve b, suggesting that the same crystalline phases are formed, and the applied magnetic field does not alter the crystalline phases. The results indicate the high magnetic field retards the crystallization kinetics of the bulk metallic glass at the condition investigated. However, the high magnetic field has no influence on the type of the crystallized phases, which can be further confirmed by similar XRD patterns of the samples annealed at higher temperature as given in Fig. 4. As shown in Fig. 4, the positions of the Bragg peaks are same for the two XRD patterns, meaning that the crystallized phases remain unchanged by the high magnetic field.

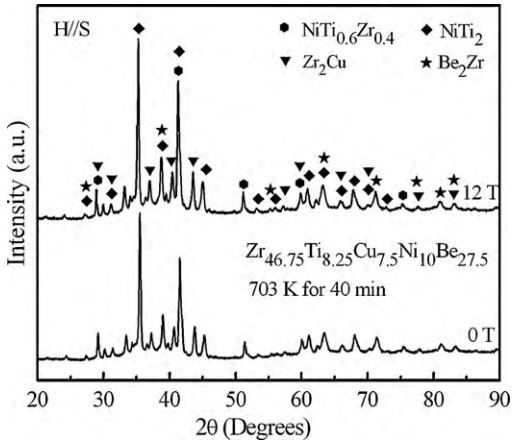

Fig. 4. XRD patterns of the $Zr_{46.75}Ti_{8.25}Cu_{7.5}Ni_{10}Be_{27.5}$ bulk metallic glass annealed at 703 K for 40 min under various intensities of the magnetic field. The direction of the magnetic field is parallel to the sample surfaces.

Crystallization of metallic glass is normally regarded as a process proceeding by nucleation and subsequent growth of crystals. The formation of nucleus is determined by the driving force for phase transformation and atomic mobility. According to the thermodynamics theory of phase transformation, the energy barrier of forming a critical nucleus size in the presence of the magnetic filed, ΔG^*, can be written as [9]

$$\Delta G^* = \frac{16\pi\sigma^3}{3[|\Delta G_v| + \frac{1}{2}H^2(\mu_2 - \mu_1)]^2} \quad (1)$$

The critical nucleus radius, γ^*, is

$$\gamma* = \frac{2\sigma}{|\Delta G_v| + \frac{1}{2}H^2(\mu_2 - \mu_1)} \quad (2)$$

where σ is the interfacial energy between crystal and glass, ΔG_v the change of bulk free energy per unit volume in process of phase transformation, H the intensity of the applied magnetic field, μ_1 and μ_2 are the magnetic permeability of the glass matrix and the crystallized phases, respectively. It is clearly seen that the energy barrier of phase transformation and the critical nucleus radius depend on the intensity of magnetic field and the magnetic permeability difference between the new crystallized phase and the glass. Hence, if $\mu_2 > \mu_1$, ΔG^* and γ^* are reduced, and nucleation is enhanced by the applied magnetic field. This is the situation where a ferromagnetic phase, for example α-Fe, is precipitated from the anti-ferromagnetic or paramagnetic amorphous matrix. However, if $\mu_2 < \mu_1$, the nucleus formation is inhibited. This could be one of the reasons why the crystallization of the $Zr_{46.75}Ti_{8.25}Cu_{7.5}Ni_{10}Be_{27.5}$ bulk metallic glass was retarded.

The primary crystallization of the bulk metallic glass requires long-range atomic diffusion due to a large composition difference between amorphous phase and its corresponding crystallization products. This implies that the crystallization is controlled by diffusion. From the crystallization kinetics theory, the steady-state homogeneous nucleation rate, I_S, is given by [3]

$$I_s = \frac{N_0 D}{a_0^2} \exp(-\frac{\Delta G^*}{k_B T}) \quad (3)$$

where D, N_0 and a_0 are the diffusivity of atoms, the number of atoms in per unit volume and the atomic diameter, respectively. While the growth rate of nucleus, U_c, can be expressed as [17].

$$U_c = a_f(D/t)^{1/2} \quad (4)$$

where t, a_f and D are time, constant and diffusivity, respectively.

Eqs. (3) and (4) suggest that the diffusion of atoms is also a key factor in nucleation and growth of the nucleus, and thereby plays an important role in crystallization of the bulk metallic glass. Youdelis et al. reported that a 3 T magnetic field retarded diffusion of copper in aluminum [18]. Nakamichi et al. found that the diffusion of carbon in γ-iron was retarded under a 6 T uniform magnetic field, and enhanced by using a negative magnetic field gradient [19]. Nakajima et al. observed that the diffusivity of nickel in titanium remains unchanged under an external magnetic field [20]. It was also found [21,22] that the magnetic field had a non-monotonic influence on the diffusivity of nickel in α-iron and Fe–%Si alloys at ferromagnetic temperatures. A maximum increase in diffusivity occurred at a weak magnetic field, and then the diffusivity was reduced with further increasing magnetic field intensity. Recently, it was reported that a 10 T high magnetic field improved the diffusion of Cu in Al–4 wt% Cu [23]. Therefore, the magnetic fields have a remarkable effect on the diffusion process of atoms, meaning that the nucleation rate and growth rate of nucleus are affected by the applied magnetic field. It is possible that the applied magnetic field to some extent retards effective diffusion of atoms, and thereby decreases the nucleation rate and the

growth rate of the nucleus. Therefore, the retarded crystallization for $Zr_{46.75}Ti_{8.25}Cu_{7.5}Ni_{10}Be_{27.5}$ bulk metallic glass under high magnetic field might be also attributed to the decrease of diffusivity of atoms.

4. Conclusions

In summary, the external high magnetic field has a strong influence on the crystallization process of the $Zr_{46.75}Ti_{8.25}Cu_{7.5}Ni_{10}Be_{27.5}$ bulk metallic glass. When the sample was annealed at 688 K, the crystallization of the bulk metallic glass has been retarded under the high magnetic field. Based on classical nucleation-growth theory, the diffusion and the difference between the magnetic permeability of the new crystallized phases and the amorphous matrix could be responsible for the crystallization retardation of the $Zr_{46.75}Ti_{8.25}Cu_{7.5}Ni_{10}Be_{27.5}$ bulk metallic glass under high magnetic field.

Acknowledgements

The work was supported by the Scientific Research Foundation for the Returned Overseas Chinese Scholars, State Education Ministry, 985 project of Northeastern University, and Fundamental Research Funds for the Central University at China.

References

[1] S. Asai, Adv. Process. Metals Mater. 5 (2006) 205.
[2] X.R. Liu, S.M. Hong, Appl. Phys. Lett. 90 (2007) 251903.
[3] Y.X. Zhuang, S.S. Yi, W.H. Wang, Mater. Trans. JIM 42 (2001) 583.
[4] Y.X. Zhuang, W.H. Wang, J. Appl. Phys. 87 (2000) 8209.
[5] S.B. Qiu, K.F. Yao, J. Non-cryst. Solid 354 (2008) 3520.
[6] J. Zhang, H.F. Zhang, M.X. Quan, Z.Q. Hu, Mater. Lett. 58 (2004) 1379.
[7] Y. Wolfus, Y. Yeshurun, I. Felner, J. Wolny, Phil. Mag. B 56 (1987) 963.
[8] Y. Otani, H. Sun, J.M.D. Coey, H.A. Davis, A. Manf, R.A. Buckley, J. Appl. Phys. 67 (1990) 4616.
[9] X.D. Wang, M. Qi, S. Yi, Scripta Mater. 51 (2004) 1047.
[10] Z.Y. Wang, H. Xu, J.S. Ni, Q. Li, B.X. Zhou, Rare Metals 25 (2006) 337.
[11] J. Fujii, S. Tsurekawa, T. Matsuzaki, T. Watanabe, Phil. Mag. Lett. 86 (2006) 113.
[12] V.A. Yardley, S. Tsurekawa, H. Fujii, T. Matsuzaki, Mater. Trans. JIM 48 (2007) 2826.
[13] H. Fujii, V.A. Yardley, T. Matsuzaki, S. Tsurekawa, J. Mater. Sci. 43 (2008) 3837.
[14] T. Zhang, X.G. Zhang, N.N. Wu, Z. Ren, F. Jia, W. Zhang, Proc. Asian-EPM 2008 (2008) 132.
[15] Y.X. Zhuang, M.H. Chen, J. Chen, J.C. He, Proc. Asian-EPM 2008 (2008) 120.
[16] Q. Wang, C.J.W. ang, T. Liu, K. Wang, J.C. He, J. Mater. Sci. 42 (2007) 10000.
[17] C. Zener, J Appl. Phys. 20 (1949) 950.
[18] W.W. Youdelis, D.R. Colton, C. Cahoon, Can. J. Phys. 42 (1964) 2217.
[19] S. Nakamichi, S. Tsurekawa, Y. Morizono, T. Watanabe, M. Nishida, A. Chiba, J. Mater. Sci. 40 (2005) 3191.
[20] H. Nakajim, S. Maekawa, Y. Aoke, M. Koiwa, Trans. Jpn. Inst. Metals 26 (1985) 1.
[21] A.V. Pokoev, D.I. Stepanov, I.S. Trofimove, V.F. Mazanko, Phys. Status Solidi (a) 137 (1993) K1.
[22] A.V. Pokoev, D.I. Stepanov, Defect Diffus. Forum 143–147 (1997) 419.
[23] L. Cui, X. Li, M. Qi, Mater. Sci. Forum 561–565 (2007) 171.